Optica Applicata, Vol. LI, No. 4, 2021
DOI: 10.37190/oa210409

Characterisation of nano-thin film GO/TiO_2 layers for Kretschmann-based surface plasmon resonance visible sensing using FDTD method

N.B. Khairulazdan[1], R. Mohamed[2], D.D Berhanuddin[1], P.S. Menon[1*]

[1]Insititute of Microengineering and Nanoelectronics (IMEN), Univesiti Kebangsaan Malaysia, Bangi, Selangor

[2]Faculty of Applied Sciences, Universiti Teknologi MARA Pahang, Pahang, Malaysia

[*]Corresponding author: susi@ukm.edu.my

Kretschmann-based surface plasmon resonance (K-SPR) is suitable for biomolecular sensing which provides label-free and quick detection results with real-time analysis. In this work, we have investigated the effect of graphene oxide (GO) with titanium dioxide (TiO_2) thin films that are placed in hybrid above metal layers such as gold (Au), silver (Ag) and copper (Cu) with the presence of chromium (Cr) as an adhesive layer. The thickness of the Au, Ag and Cu metal thin films were optimized to 40, 30 and 30 nm, respectively, with a fixed thickness of GO of 2 nm and TiO_2 of 1.9 nm. The sensing was evaluated for SPR excitation at three different visible wavelengths of 633, 670 and 785 nm. The performance of sensing was analyzed based on the reflectance intensity and full -width at half-maximum (FWHM) of the spectrum using the finite-difference time-domain (FDTD) method. The sensitivity was calculated for analyte sensing in dielectric mediums of air *versus* water. The sensitivity increment percentage (%ΔS) was determined when comparing analyte detection using Cr/metal and Cr/metal/GO/TiO_2 sensor structures. The highest sensitivity of 94.51 deg/RIU was achieved for Cr/Cu/GO/TiO_2 K-SPR sensor at 633 nm wavelength.

Keywords: surface plasmon resonance, FDTD, titanium dioxide, graphene oxide, Kretschmann, biosensor.

1. Introduction

Surface plasmon resonance (SPR) is well-known as one of the powerful optical detection methods for real-time biomolecular detection in various applications. In this work, we use the Kretschmann configuration of the SPR which provides sensing analysis in a label-free environment; either in liquid or gas medium. The SPR process occurs when light which passes through a glass prism is reflected upon contact with a nanofilm metal surface layer and collected into a photodetector. Then, at a certain incident angle known as the resonance angle, when the wave vector of the optical light is in tandem with the wave vector of the electron gas field in the metal film of the sensor structure, a plasmonic

field is formed above the nano-metal film. Any changes in the dielectric layer above the nano-metal film cause changes in the reflected light. Therefore, the Kretschmann configuration is the best method to apply for plasmon excitation. The biomolecular interaction can be determined by measuring the SPR resonant angle shift during sensing [1, 2]. The sensitivity of the SPR sensor can be improved by using nanoparticles in the nano-thin film. But at the same time, we have to consider the nanoparticle and the thickness of each layer of the thin film so that we can maximize the efficiency of detection. Next, if we want to study the ability of charge carrier to absorb and emit, photoluminescence (PL) measurement can be used [3–5]. The photoluminescence emission occurs due to the phenomena of recombination of excited electron-hole pair. When the recombination rate is low, the emission intensity is also low [6]. Therefore, SPR phenomenon can then be realised upon the improvement of photoreaction by PL emission. Each layer of the Kretschmann-based surface plasmon resonance (K-SPR) sensor has its properties to make better detection and emission. Graphene oxide (GO) can be a suitable layer because it has a high surface area that can help the absorption of light and also prevent oxidation from occurring. In this work, titanium dioxide (TiO_2) was chosen to be the structure underneath GO because this type of metal oxide will provide a strong plasmonic field improvement with localization and allows controlling light dispersion and absorption [7]. The bandgap of GO is 0 eV so TiO_2 functions to reflect light at a maximum intensity which in turn interacts directly to the metal surface [8]. TiO_2 has excellent chemical stability which makes it a suitable material for biosensor detection and because of that, it will improve the PL spectra intensity. PL spectra can be one of the best measurements to analyze the performance of TiO_2 as a biosensor because it shows the shift in conductivity. According to a previous study, TiO_2 was used on a glass substrate for SPR detection and this was followed by the application of PL spectra measurements in an effort to design an immunosensor for *Salmonella* detection. The sensitivity is compared between glass/TiO_2 sensor and glass/TiO_2/anti-S-Ab antibodies where *Salmonella* antigens show a shifted resonant angle and increasing intensity of PL [9]. Therefore, this kind of hybrid thin film comprising of GO/TiO_2 is needed to enhance sensing in many fields especially in biomedical sensing.

2. Methodology

To perform the simulation model of the K-SPR, finite-difference time-domain (FDTD) from Lumerical was used. The suitable and critical choice of the metal film needs to be considered for the simulation process. The wavelengths that were used are 633, 670 and 785 nm based on the Kretschmann configuration. The structure of the thin film consists of five layers which are soda-lime glass (BK7), chromium (Cr) adhesion layer, metal layers such as gold (Au), silver (Ag) and copper (Cu) that are placed in hybrid with a graphene oxide (GO) layer and titanium dioxide (TiO_2) as the outermost layer of the thin film. This is shown schematically in Fig. 1.

Generally, the incident angle is set to range from 36 to 80 degrees so that when the y component of the incident light wave vector corresponds to the wave vector of the elec-

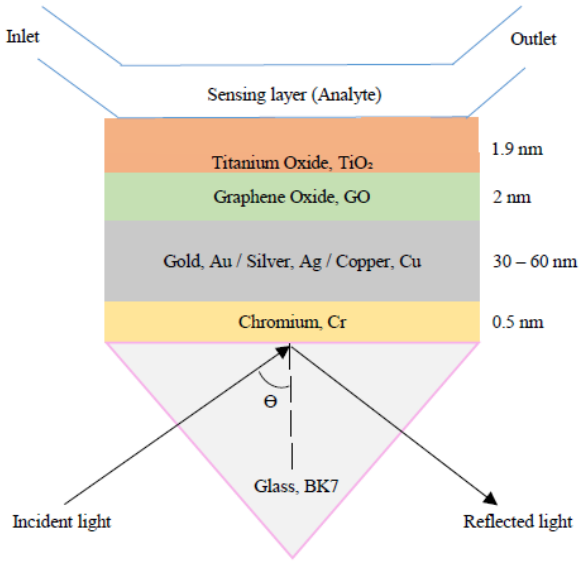

Fig. 1. Schematic configuration of SPR based on the Kretschmann method.

tron gas at the surface of the metal thin film; thus exciting the SPR mode. The SPR parameter that is desired to be known is the resonance angle θ_{res} where minimum reflection intensity occurs as well as the SPR spectra's full-width at half-maxima (FWHM). The calculation of FWHM relates to the value of upper resonant angle minus the lower resonant angle at the half maximum reflection of the SPR spectra [10]. Thus, when the FWHM value is smaller, it means that the spectrum is narrower and has a deeper sensing peak which is suitable for sensitive detection. After that, to further analyse the performance of the sensors, the sensitivity S is determined as the ratio of the difference between the two resonances angles θ_{res} of different analytes to the change in the refractive index of the analytes [11]. In this work, we evaluate the sensitivity of the sensor from the dielectric medium of air with refractive index of $n = 1$ to the refractive index of water, $n = 1.33$. The larger the SPR curve shift of two different mediums, the higher the sensitivity value and thus the performance of the sensor is greater [12].

3. Results and discussion

3.1. Effect of adding GO and TiO_2 thin film

From the simulation results based on FDTD analysis, we assume that maximum intensity of light is absorbed at resonance condition to excite the surface plasmon wave (SPW) that transmits along the interface between the metal layer and the dielectric medium. Figure 2**a** shows the comparison of intensity slope for Au with a thickness of 40 nm underneath GO/TiO_2 layers at wavelength 633, 670 and 785 nm. The narrowest slope is observed for wavelength 785 nm and the reflectance intensity is maximum at wavelength 633 nm. Next, Fig. 2**b** indicates that the optimum thickness of Ag is 30 nm

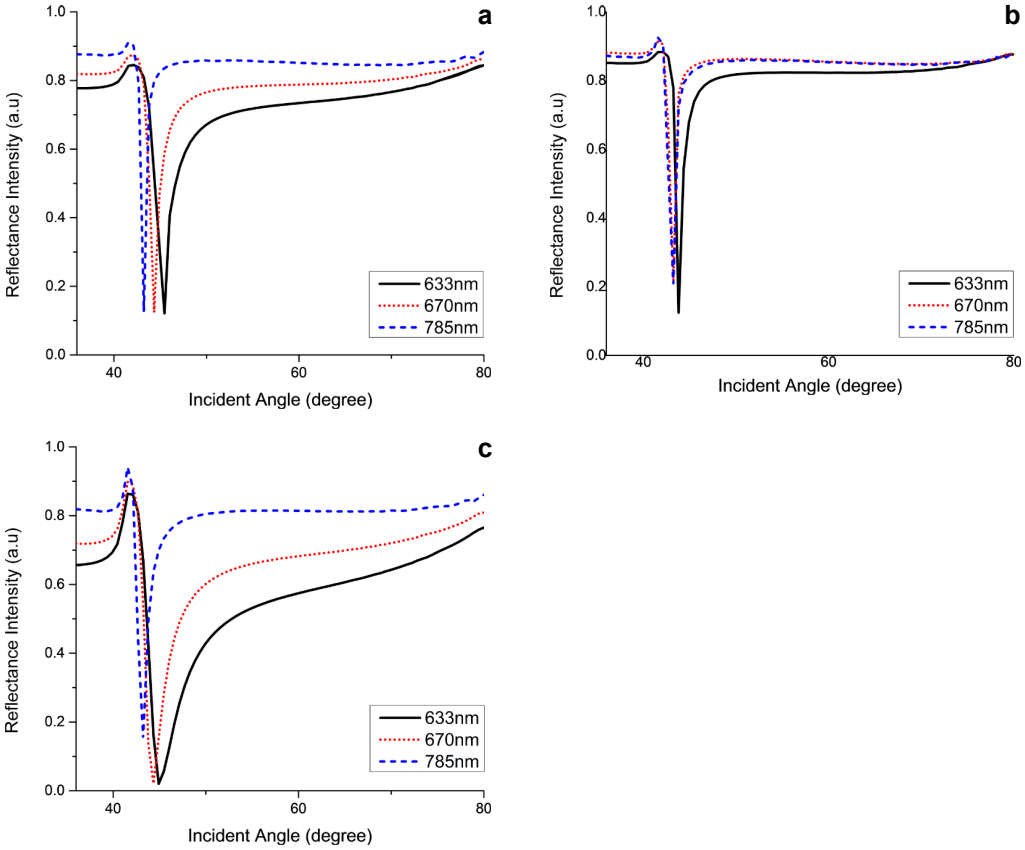

Fig. 2. The SPR simulation at wavelength 633, 670 and 785 nm for (**a**) Au with thickness of 40 nm, (**b**) Ag with thickness of 30 nm, and (**c**) Cu with thickness of 30 nm.

underneath GO/TiO_2 layers having the most reflectance intensity occurring at wavelength 633 nm. Among all the metal used, Fig. 2**c** proves that Cu with thickness 30 nm has the most absorbed light with the highest intensity at wavelength 633 nm but the minimum FWHM value is at wavelength 785 nm.

From Table 1, at wavelength 633 nm we found out the best R_{min} is when metal Cu is layered with GO/TiO_2 with 0.0202730 at 44.91°. Metal Ag has the lowest FWHM value which is 0.9744°. Other than that, Table 2 tabulated based on 670 nm shows that GO/TiO_2 hybrid with metal Cu has then lowest R_{min} value with 0.0208869 at 44.35° and when GO/TiO_2 hybrid with metal Ag has the best FWHM value with 0.7859°. Table 3 also indicated the same metal Cu with the best R_{min} value 0.1528170 at 43.21° and Au with the lowest FWHM value 0.9450 at wavelength 785nm. Thus, from Tables 1, 2, and 3 for 633, 670 and 785 nm, respectively, the overall observation at each wavelength for every metal: Au, Ag and Cu indicates that R_{min} reduces when

T a b l e 1. Resonance angle, R_{min} and FWHM at wavelength 633 nm for Au with thickness of 40 nm, Ag with thickness of 30 nm and Cu with thickness of 30 nm underneath GO/TiO_2 layers.

Structure	θ_{res} [deg]	R_{min}	θ_{FWHM} [deg]
Au/GO	44.3544	0.1303291	1.8008
Au/GO/TiO_2	44.4547	0.1212110	2.1025
Ag/GO	43.7975	0.1535235	0.8895
Ag/GO/TiO_2	43.7975	0.1247598	0.9744
Cu/GO	44.3544	0.0388928	5.6600
Cu/GO/TiO_2	44.9114	0.0202730	7.0084

T a b l e 2. Resonance angle, R_{min} and FWHM at wavelength 670 nm for Au with thickness of 40 nm, Ag with thickness of 30 nm and Cu with thickness of 30 nm underneath GO/TiO_2 layers.

Structure	θ_{res} [deg]	R_{min}	θ_{FWHM} [deg]
Au/GO	43.7975	0.1320886	1.1472
Au/GO/TiO_2	44.3544	0.1240670	1.2543
Ag/GO	42.6835	0.2652990	0.6049
Ag/GO/TiO_2	43.2405	0.2182750	0.7859
Cu/GO	43.7975	0.0273308	3.0980
Cu/GO/TiO_2	44.3544	0.0208869	3.5144

T a b l e 3. Resonance angle, R_{min} and FWHM at wavelength 785 nm for Au with thickness of 40 nm, Ag with thickness of 30 nm and Cu with thickness of 30 nm underneath GO/TiO_2 layers.

Structure	θ_{res} [deg]	R_{min}	θ_{FWHM} [deg]
Au/GO	43.2405	0.2307459	0.8320
Au/GO/TiO_2	44.2405	0.1263640	0.9450
Ag/GO	42.6835	0.3569870	0.6729
Ag/GO/TiO_2	43.2405	0.2076880	0.9860
Cu/GO	42.6835	0.1915660	1.6144
Cu/GO/TiO_2	43.2405	0.1528170	1.7440

we add TiO_2 on top of GO. The pattern of FWHM also becomes deeper and narrower as the wavelength increases. Also, the resonance angle shifts toward the bigger value by the addition of the TiO_2 in the structure. Hence, TiO_2 shows a huge difference in the sensor efficiency that causes much light to be absorbed.

3.2. Sensitivity measurement

The sensitivity was calculated for the addition of GO/TiO_2 layer on top of metal layers through angular interrogation. Fundamentally, the sensor is applied with the reference medium which is dielectric medium also known as air with refractive index, $n = 1$. After that, we identify the sensitivity of the sensor using water with a refractive index of

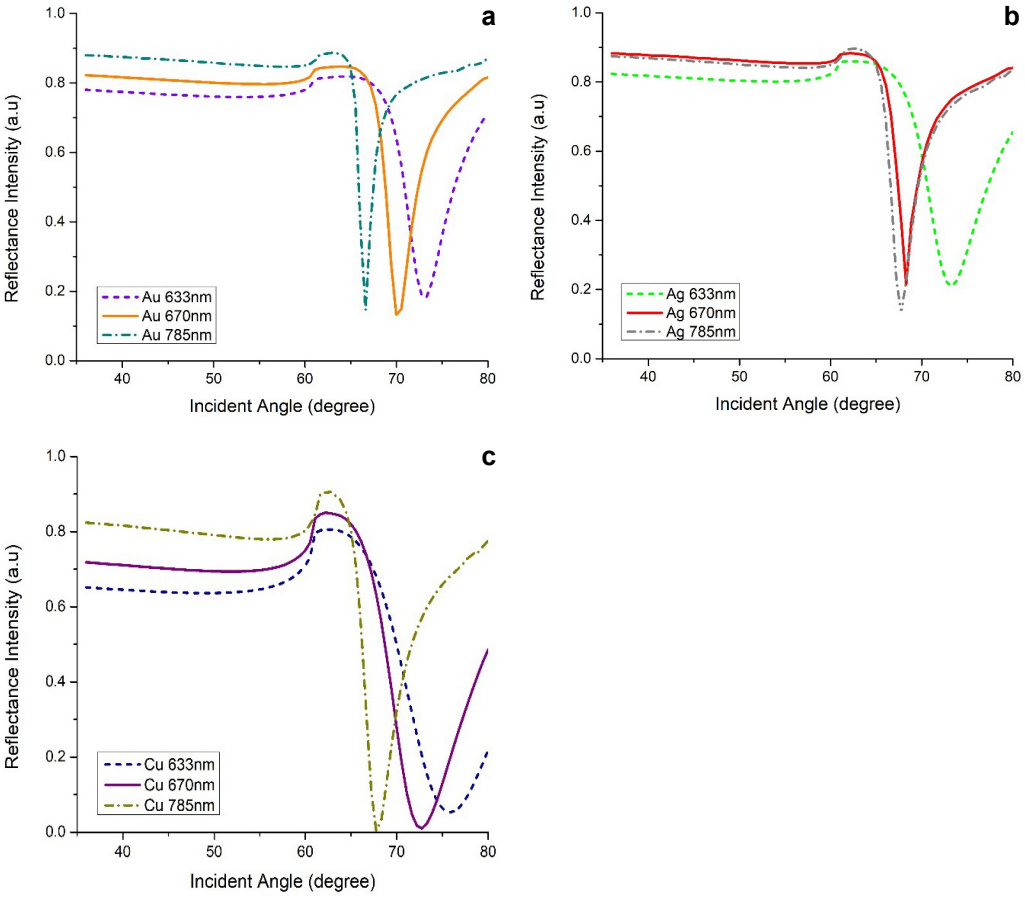

Fig. 3. The sensitivity shifted of SPR-based sensor of metal (**a**) Au with thickness of 40 nm, (**b**) Ag with thickness of 30 nm (**c**), and Cu with thickness of 30 nm with the sensing layer exposed to water, $n = 1.33$ at wavelength 633, 670 and 785 nm.

$n = 1.33$. The analyses of Figures 3**a**–3**c** are based on: the more shifted the resonance angle on the graph from air to water, the better the sensitivity of the sensor of each wavelength 633, 670 and 785 nm.

From Table 4, the presence of GO/TiO_2 layers on top of Cr/Au gives better-shifted value compared to the conventional Cr/Au from air to water at 633, 670 and 785 nm. The sensitivity of GO/TiO_2 layer with metal Au at wavelength 633, 670 and 785 nm increased from 81.01 to 92.83 deg/RIU, from 86.45 to 89.46 deg/RIU, and from 72.57 to 77.64 deg/RIU, respectively. Next, the sensitivity of metal Ag underneath GO/TiO_2 also rose from 77.64 to 89.45 deg/RIU, from 70.89 to 75.95 deg/RIU, and from 70.89 to 74.26 deg/RIU at wavelength 633, 670 and 785 nm, accordingly. For metal Cu/GO/TiO_2, the sensitivity at 633 nm expands rapidly from 82.70 to 94.51 deg/RIU, at

T a b l e 4. The sensitivity and sensitivity of different percentages at wavelength 633, 670 and 785 nm.

Wavelength [nm]	Structure	Sensitivity S [deg/RIU]	%ΔS
633	Cr/Au	81.01	12.73
	Cr/Au/GO/TiO_2	92.83	
	Cr/Ag	77.64	13.20
	Cr/Ag/GO/TiO_2	89.45	
	Cr/Cu	82.70	12.50
	Cr/Cu/GO/TiO_2	94.51	
670	Cr/Au	86.45	3.35
	Cr/Au/GO/TiO_2	89.45	
	Cr/Ag	70.89	6.66
	Cr/Ag/GO/TiO_2	75.95	
	Cr/Cu	82.70	3.93
	Cr/Cu/GO/TiO_2	86.08	
785	Cr/Au	72.57	6.53
	Cr/Au/GO/TiO_2	77.64	
	Cr/Ag	70.89	4.54
	Cr/Ag/GO/TiO_2	74.26	
	Cr/Cu	70.89	4.54
	Cr/Cu/GO/TiO_2	74.26	

670 and 785 nm increases slightly from 82.70 to 86.08 deg/RIU and from 70.89 to 74.26 deg/RIU, respectively. The shift of the resonance angle happened because of the light travel from one medium to other.

4. Conclusion

As a summary, in this work for the first time to our knowledge, we have determined the presence of GO/TiO_2 thin films that are placed in hybrid form above noble metal nano-layers such as gold (Au), silver (Ag) and copper (Cu) using K-SPR sensor for three different wavelengths. The value of R_{min} and FWHM for Au with optimum thickness of 40 nm layer below GO/TiO_2 were 87.88%, 2.1025°; 87.59%, 1.2543°; 87.37%, 0.9450° at wavelengths of 633, 670 and 785 nm, respectively. Next, the value of R_{min} and FWHM for Ag with optimum thickness of 30 nm below the GO/TiO_2 were 87.52%, 0.9744°; 78.17%, 0.7859°; 79.23%, 0.9860° at wavelengths of 633, 670 and 785 nm, respectively. Also, the value of R_{min} and FWHM for Cu with optimum thickness of 30 nm below the GO/TiO_2 were 97.97%, 7.0084°; 97.91%, 3.5144°; 84.72%, 1.7440° at wavelengths of 633, 670 and 785 nm, respectively. The %ΔS for metal Au, Ag and Cu on thin film TiO_2 are 12.73%, 13.20% and 12.50%, respectively, at the best wavelength of 633 nm. Among all the metals used in wavelength 633 nm, silver (Ag) with the

thickness 30 nm underneath GO/TiO_2 layer shows the highest sensitivity improvement of 13.20% *versus* the sensor without the presence of the GO/TiO_2 layers. The K-SPR structure with the highest sensitivity is 94.51 deg/RIU which was achieved for Cr/Cu/GO/TiO_2 K-SPR sensor at 633 nm wavelength which is recommended for biomolecular detection.

Acknowledgment – This work was supported by the Malaysian Ministry of Education and Universiti Kebangsaan Malaysia using fundamental research grants FRGS/1/2019/STG02/UKM/02/8 and DIP-2016-022. Institute of Microengineering and Nanoelectronics (IMEN), UKM and Universiti Teknologi MARA (UiTM) are also acknowledged for the support.

References

[1] SAID F.A., MENON P.S., KALAIVANI T., MOHAMED M.A., ABEDINI A., SHAARI S., MAJLIS B.Y., RETNASAMY V., *FDTD analysis of structured metallic nanohole films for LSPR-based biosensor*, [In] *2015 IEEE Regional Symposium on Micro and Nanoelectronics (RSM)*, Kuala Terengganu, Malaysia, 2015, DOI: 10.1109/RSM.2015.7355024.

[2] MENON P.S., SAID F.A., GAN S.M., MOHAMED M.A., ZAIN A.R.M., SHAARI S., MAJLIS B.Y., *High sensitivity Au-based Kretschmann surface plasmon resonance sensor for urea detection*, Sains Malaysiana **48**(6), 2019, pp. 1179–1185, DOI: 10.17576/jsm-2019-4806-04.

[3] HORIUCHI Y., SHIMADA M., KAMEGAWA T., MORI K., YAMASHITA H., *Size-controlled synthesis of silver nanoparticles on Ti-containing mesoporous silica thin film and photoluminescence enhancement of rhodamine 6G dyes by surface plasmon resonance*, Journal of Materials Chemistry **19**(37), 2009, pp. 6745–6749, DOI: 10.1039/b910474g.

[4] BERHANUDDIN D.D., LOURENCO M.A., GWILLIAM R.M., HOMEWOOD K.P., *Photoluminescence study of the optically active, G-centre on pre-amorphised silicon by utilizing ion implantation technique*, [In] *2016 IEEE International Conference on Semiconductor Electronics (ICSE)*, 2016, pp. 256–259, DOI: 10.1109/SMELEC.2016.7573640.

[5] BERHANUDDIN D.D., LOURENCO M.A., GWILLIAM R.M., HOMEWOOD K.P., *The effect of temperature to the formation of optically active point-defect complex, the carbon G-centre in pre-amorphised and non-amorphised silicon*, IOP Conference Series: Materials Science and Engineering **384**(1), 2018, article 012062, DOI: 10.1088/1757-899X/384/1/012062.

[6] YANG Y., LIU E., DAI H., KANG L., WU H., FAN J., HU X., LIU H., *Photocatalytic activity of Ag-TiO_2-graphene ternary nanocomposites and application in hydrogen evolution by water splitting*, International Journal of Hydrogen Energy **39**(15), 2014, pp. 7664–7671, DOI: 10.1016/j.ijhydene.2013.09.109.

[7] SAID F.A., MENON P.S., SHAARI S., MAJLIS B.Y., *FDTD analysis on geometrical parameters of bimetallic localized surface plasmon resonance-based sensor and detection of alcohol in water*, International Journal of Simulation: Systems, Science and Technology **16**(4), 2015, pp. 6.1–6.5, DOI: 10.5013/IJSSST.a.16.04.06.

[8] MENON P.S., MULYANTI B., JAMIL N.A., WULANDARI C., NUGRUHO H.S., GAN S.M., ABIDIN N.F.Z., HASANAH L., PAWANTO R.E., BERHANUDDIN D.D., *Refractive index and sensing of glucose molarities determined using Au-Cr K-SPR at 670/785 nm wavelength*, Sains Malaysiana **48**(6), 2019, pp. 1259–1265, DOI: 10.17576/jsm-2019-4806-13.

[9] VITER R., TERESHCHENKO A., SMYNTYNA V., OGORODNIICHUK J., STARODUB N., YAKIMOVA R., KHRANOVSKYY V., RAMANAVICIUS A., *Toward development of optical biosensors based on photoluminescence of TiO_2 nanoparticles for the detection of Salmonella*, Sensors and Actuators B: Chemical **252**, 2017, pp. 95–102, DOI: 10.1016/j.snb.2017.05.139.

[10] ZHENG X., *The optics and applications of graphene oxide*, PhD Thesis, Swinburne University of Technology, 2016.

[11] Menon P.S., Jamil N.A., Gan S. M., Zain A.R.M., Hewak D.W., Huang C.-C., Mohamed M.A., Majlis B.Y., Mishra R.K., Raghavan S., Bhat N., *Multilayer CVD-graphene and MoS_2 ethanol sensing and characterization using Kretschmann-based SPR*, IEEE Journal of the Electron Devices Society **8**, 2020, pp. 1227–1235, DOI: 10.1109/JEDS.2020.3022036.

[12] Gan S.M, Menon P.S., Hegde G., *ZnO for performance enhancement of surface plasmon resonance biosensor: a review*, Materials Research Express **7**(1), 2020, article 012003, DOI: 10.1088/2053-1591/ab66a7.

Received September 15, 2020